

GAIVBE技法에 의한 低溫 Al₂O₃ on Si 薄膜의 形成과 電氣的 特性에 관한 研究

논문
8-3-9

A Study on the Electrical Characteristics and the Growth of Al₂O₃ Film on Si with Low Temperatures by GAIVBE Technique

성만영*, 김태익*, 문병무*, K.V.Rao**, 박성희***

(Man-Young Sung · Tae-Ik Kim · Byoung-Moo Mun · K.V.Rao · Sung-Hee Park)

요 약

本 論文에서는 Al₂O₃薄膜을 GAIVBE(Gas Assisted Ionized Vapour Beam Epitaxy)技法에 의해 低溫에서 300~1,400Å의 두께로 成長하여 그 條件을 提示하였다.

아울러 Al-Al₂O₃-Si의 MOS 構造를 製作하여 電氣的 特性을 考察하고 그 結果를 分析, 提示하므로써 GAIVBE技法에 의해 低溫으로 形成된 Al₂O₃膜의 活用 可能性을 報告하였다.

한편, 本 研究에서 製作한 Al₂O₃薄膜의 抵抗率은 膜의 두께 100~1,000Å인 試料製作에서 10⁸ohm-cm와 10¹³ohm-cm로 測定되었고, 比誘電率은 8.5~10.5, 絶緣破壞強度 6~7MV/cm(+바이어스)와 11~12MV/cm(-바이어스)이었다.

1. INTRODUCTION

The use of silicon dioxide(SiO₂) as an insulator has become so widespread in the microelectronics industry. However, since SiO₂ does not satisfy all criteria for an ideal technological insulator, there have been many investigations for some years by numerous researchers searching for possible alternative insulators.^{1~6)}

Among those which have been seriously studied are phosphosilicate glass(PSG), silicon nitride (Si₃N₄), and aluminum oxide(Al₂O₃). Aluminum

oxide has some unique advantage over SiO₂ which makes it promising: greater resistance to ionic motion,⁷⁻⁹⁾ greater radiation hardness,⁷⁾ the possibility of obtaining low threshold voltage MOS FETs, and the possibility of use in nonvolatile memory devices. Balk²⁾ has proposed a set of criteria to be employed in the selection of insulators either instead of, or in conjunction with SiO₂: 1)high dielectric constant, 2)high breakdown strength(>1MV/cm), 3)an effective barrier against contaminants such as alkali ions and moisture, 4)etchable in liquid etchants at or near room temperature, 5)stable electrical properties when used as gate insulator in FET, 6)controllable electrical properties when used as nonvolatile memory elements.

Many of these requirements are fulfilled very well by Al₂O₃. Al₂O₃ is believed to be more resistant to ionic penetration than SiO₂.

* 고려대학교 전기공학과

** Royal Institute of Technology Dept.of Condensed Matter Physics

*** 호서대학교 전자공학과

접수일자 : 1994년 12월 6일

심사완료 : 1995년 3월 6일

Insulating films on III-V compounds must be deposited at lower temperature than 400°C owing to the volatility of V group elements.

This is the reason that the formation of insulators by a high temperature process is not applicable. Therefore low temperature and no damage deposition process of insulating films are strongly required.

Low temperature deposition of crystalline insulating films on various kinds of semiconductor substrates are also of great interest in formation of MIS structures which can be applied to fabricate three dimensional integrated circuits. So we have Al₂O₃ films deposited by Gas Assisted and Ionized Vapour Beam Epitaxy Technology(GAIVBE) at low temperature.¹⁰⁻¹¹⁾ In this paper, details of the film deposition system and fundamental characteristics of the Al-Al₂O₃-Si structures were described and the dielectric breakdown of Al₂O₃ was studied.

2. SAMPLE PREPARATION

2-1. Al₂O₃/Si Structure Preparation

In our experiments, both n and p type silicon wafers of 4~6 ohm-cm resistivity used.

The substrates were first cleaned with ammonia hydrogen peroxide-ammonia HCl. Films were deposited at different conditions (ionization currents, acceleration voltage and substrate temperature) and films were also deposited on Si(111) for MOS structures.

This technique is based on the formation of aluminum oxide when molten Al is evaporated in an oxygen atmosphere. Details of the GAIVBE system are described in Fig.1.

Deposition chamber was evacuated by diffusion pump with cooled trap until 1.0×10^{-7} torr. and Al evaporant(99.999%) was heated to 1,200~1,500°C in the BN or Quartz crucible with nozzle of 0.5~2mm in diameter and 1~3mm in length. Typical deposition conditions are listed in table 1.

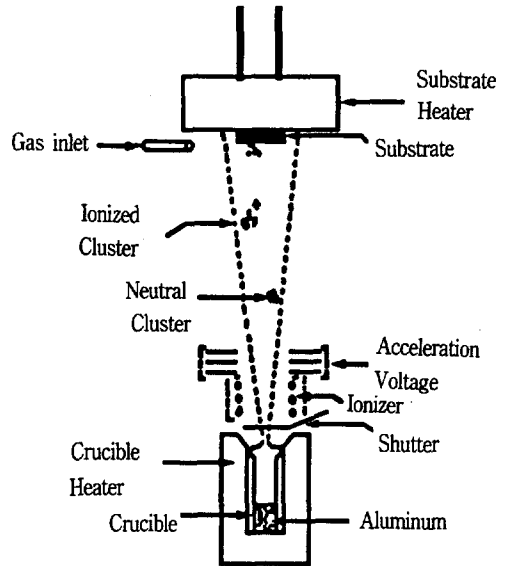


Fig 1. Schematic Diagram of the Gas Assisted and Ionized Vapour Beam Epitaxy System.

Table 1. Deposition conditions for Gas Assisted and Ionized Vapour Beam Epitaxy techniques.

Vacuum Pressure with O ₂ Gas	1×10^{-4} torr
Substrate Temperature	150~650°C
Acceleration Voltage	0~5kV
Ionizer Current	0~1.5A
Nozzle Size	0.4~2.5mm
Nozzle Length	(1~40) × Nozzle Size
Crucible Temperature	1,200~1,500°C

Oxygen is then allowed into the vacuum chamber with the aid of a needle valve control near the substrate holder. When the vacuum pressure reaches 1.5×10^{-4} torr, the needle valve control is set such that equilibrium is reached between the incoming oxygen and the outgoing gases. During the evaporation Al and oxygen molecules collide, increasing the aluminum oxide content of the evaporating gases. The efficiency of this collision process is determined

by the capture cross sections of the particles involved and the partial pressure of the oxygen gas.

It is therefore very important to allow the oxygen to flow through the system prior to evaporation so that the percentage of oxygen gas in the bell jar or near the substrate reaches a saturation value. As the Al_2O_3 is depositing, a shutter protecting the substrates from preparatory evaporations is opened. The shutter is then closed when the desired thickness of Al_2O_3 has been deposited on the substrate. After the oxide formation the substrate is placed in an oven at 150°C for the post baking of a few min. This step is necessary to complete the oxide formation of Al molecules which did not interact with oxygen molecules during the evaporation.

In our experiments, the Al_2O_3 thicknesses were about $300\sim 1,400\text{\AA}$. The oxide thicknesses were determined ellipsometrically (DHA-OLEllipsometer) and varied by about 2% over the wafer for 450\AA oxides and by as much as 5% over the wafer for the 900\AA oxides. The samples had a heat treatment of $1,000^\circ\text{C}$ for 30 minutes for annealing. As soon as possible, after the heat treatment, Al metallurgy is applied in the form of dots, in diameter, by evaporation followed by a post metallization annealing treatment of 400°C for 30 minutes in N_2 . All samples received a back contact of aluminum. The front contact was metallized with dot of aluminum. The samples used in our experiments had contact of thickness $1,000\text{\AA}$ with 0.080cm diameter circular geometries and area $2\times 10^{-2}\text{cm}^2$ (square geometries).

The index of refraction was determined to vary from 1.68 to 1.73 over the entire set of wafers by Abeles Measurement System.

The relative dielectric constant was calculated by measuring the diameter of the dot under the optical microscope. The relation

$$C = \frac{\epsilon_r \epsilon_o A}{L} = \frac{\epsilon_r \epsilon_o}{L} \left(\frac{\pi}{4} d^2 \right)$$

was then used to find the relative dielectric constant ϵ_r where ϵ_o =permittivity of vacuum $=8.85\times 10^{-14}\text{F/cm}$, L =oxide thickness and d =diameter of metal dot on the Al_2O_3 .

The data taken over a number of capacitors on the same and on different wafers, gave a value of ϵ_r ranging from 8.5 to 10.5. The resistivity of Al_2O_3 films varies from 10^8 ohm-cm for films less than 100\AA to 10^{13} ohm-cm for films on the order of $1,000\text{\AA}$. Low temperature Al_2O_3 formation is performed by GAIVBE technique. In our experiments, optimum conditions were 1kV (acceleration voltage), 800mA (Ionizer current) and 400°C (substrate temperature). Electrical characteristics of Al_2O_3 films deposited at these conditions was measured and analyzed.

2.2. Measurement Techniques

The trapping of charge in the oxide is most readily observable in the time evolution of the C-V curves. The experimental procedure for obtaining these curves was as follows. The initial C-V curve was recorded by sweeping the sample from accumulation to inversion and back to accumulation. Then, the high field bias was applied for a given time. The C-V curve was then recorded, again sweeping from accumulation to inversion and back.

The electron current is induced in the Al_2O_3 using avalanche injection from the Si. A feedback circuit is used between the output of the electrometer and the 500kHz square wave generator to control the amplitude of the square waves and keep the current in the Al_2O_3 constant at a value that is present as desired.

As trapping occurs, the square wave amplitude is automatically increased to compensate for the effect of the trapped charge. The square waves are interrupted periodically to measure automatically the flatband voltage as a means for monitoring the trapped charge build up in Al_2O_3 . In the course of a typical run $400\sim 600$ measurements are made. These data are fed into a computer and results are analyzed to

provide information concerning the trap cross sections and the traps densities. The computer program can resolve two different traps if their cross sections are separated by at least a factor of 2. The analysis of the results follows the same procedure followed by Di Maira.⁴⁾

Observations of breakdown phenomena were made in several ways.

The time to breakdown was recorded by photographing the oscilloscope trace of the current vs. time waveform or by recording the output of the Keithley 415 Electrometer on the HP 7044A X-Y recorder.

Inspection of breakdown damage was using Microscope, and was recorded on Polaroid Film. Details of the results of dielectric breakdown studies were described in this paper.

3.EXPERIMENTAL RESULTS

One method of studying dielectric breakdown is to apply a constant high voltage to the sample and observe the I-t behavior. Fig.2 shows the behavior of the current for an applied bias of +22V on a 450Å film of Al_2O_3 with Al metallization and n-Si substrate. After the application of bias the current first rises rapidly to a peak(which is much greater than that shown in Fig.2 because of the X-Y recorder's relatively slow response time) and then decays monotonically. At t=80s, we see a sharp rise in the current, corresponding to electrical breakdown of the Al_2O_3 .

This is a typical result obtained with Al electrodes. In some samples, we observed a small fluctuation in current prior to breakdown, similar to what Tsujide et al. reported.¹²⁾

We were not able to see this fluctuation in all cases. Fig.3 shows a typical I-t curve obtained with a gold electrode. The spikes in the curve correspond to self-quenching breakdowns (SQBD). Note that the SQBD's tend to occur with greater frequency as t increases.

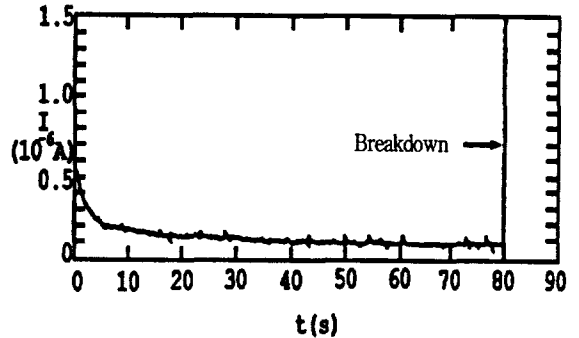


Fig.2. Current(I) vs. time(t) for +22V bias on Al-(450 Å) Al_2O_3 -n-Si

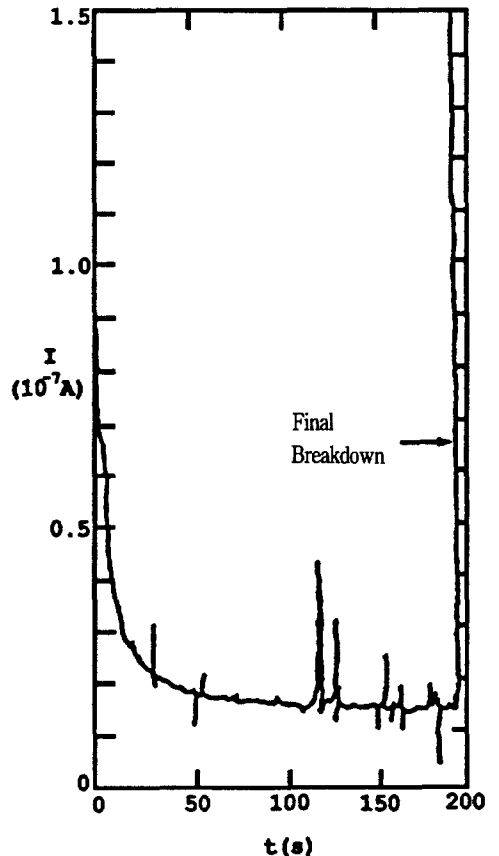


Fig.3. Typical current decay for Al-(450 Å) Al_2O_3 -n-Si for +27.5V bias

Although we have found it easy to produce SQBD's in samples with Au electrodes, we have never observed them in samples with Al electrodes.

The final breakdown is not necessarily a shorting breakdown in all cases, but might be described as the switching from a low-conductivity to a high conductivity state.

This can be seen in Fig.4, which show C-V curves taken before and after the breakdown event, for negative bias applied to a p-Si substrate, with Al electrode. Note the initial increase in ΔV_{FB} up to 25~50s, followed by a decrease, shown by the curves moving to the left. This is a typical result obtained with negative bias. Note that there is a stretchout of the C-V curve as well as a shift after breakdown. We have observed both positive and negative shifts with negative bias.

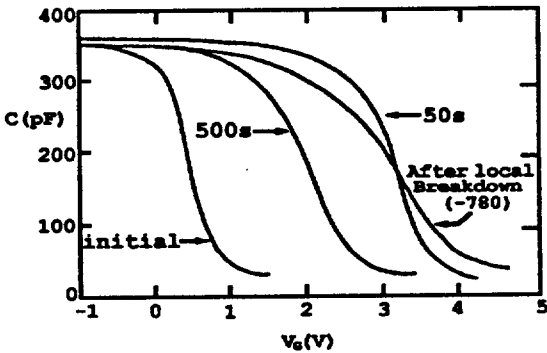


Fig.4. Typical pre- and post-breakdown C-V curves for 20V bias on Al-(450Å) Al₂O₃-p-Si

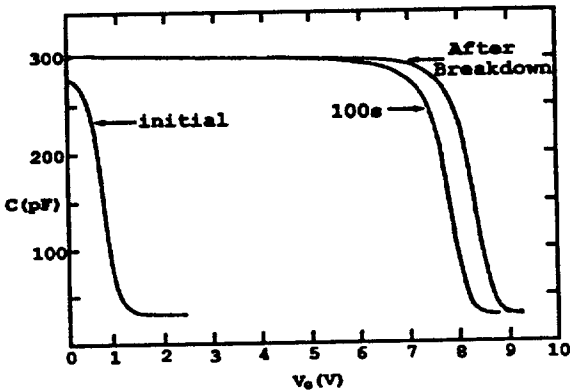


Fig.5. Typical pre- and post-breakdown C-V curves for +18V bias on Al-(450Å) Al₂O₃-p-Si under incandescent illumination

Fig.5 shows the C-V curves before and after breakdown for positive bias on p-Si samples. Incandescent illumination was used to maintain an inversion layer.

Fig.6 shows the pre- and post-breakdown curves for an n-Si sample positively biased with Al electrode. The hump of the post-breakdown curve is due to the capacitance meter being "fooled" by the large leakage current. Nevertheless, we see that the post-breakdown curve is shifted back almost to the initial C-V curve.

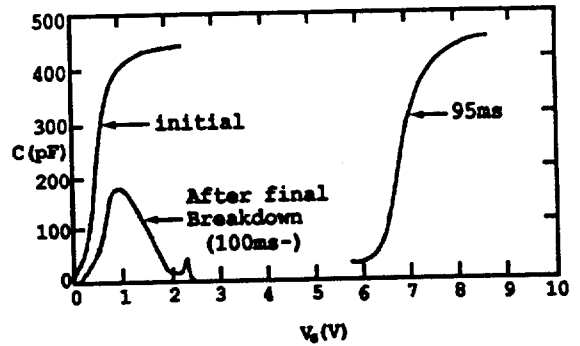


Fig.6. Typical pre- and post-breakdown C-V curves for +22V bias on Al-(450Å) Al₂O₃-n-Si

Fig.7 shows the typical results for negative bias applied to a Au-plated oxide. Here again we observe a negative flat band shift immediately following breakdown. In this case

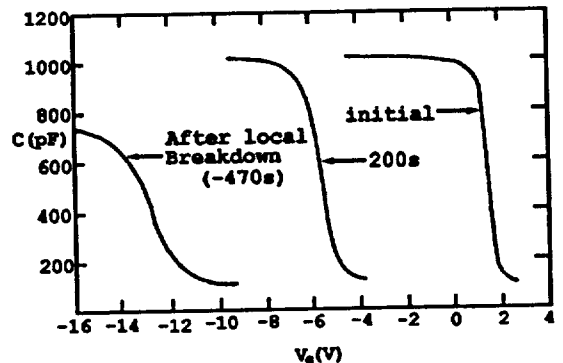


Fig.7. Typical pre- and post-breakdown C-V curves for -32.5V bias on Al-(450Å) Al₂O₃-p-Si

there is also distortion of the C-V curve.

The determination of the breakdown strength of Al₂O₃ is not straightforward. The usual method of applying a voltage ramp to the MOS capacitor and measuring the voltage at which the sample breakdown is not adequate. Because of charging effects, the breakdown voltage measured by the ramp technique will depend on the ramp rate: the greater the ramp rate, the greater will be the breakdown voltage. An alternative method is to apply a fixed bias and measure the time to breakdown. By making a series of such measurements at different biases, we obtain curves such as are displayed in Fig.8. As the curves do not approach a limiting field as $t \rightarrow \infty$, we shall define the breakdown field at an arbitrary time, such as $t=10^3$ s. The quoted breakdown field is the average field in the oxide, not the maximum field. Note also that there is a difference of 1MV/cm in the breakdown field for negative bias and for positive bias. Observation of Fig.8 shows that the breakdown field is about 4.5MV/cm for positive bias and about 5MV/cm for negative bias on p-Si.

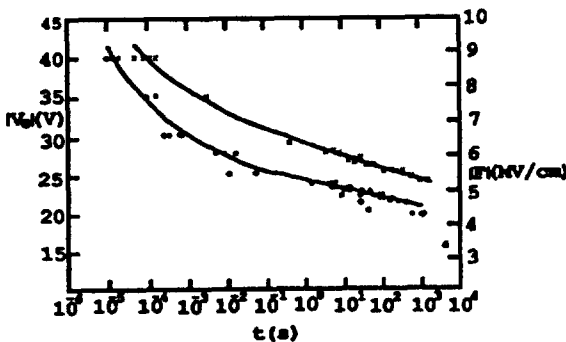


Fig.8. Applied field, F vs. time to breakdown, t
 ● : positive bias on Al-(450 Å)Al₂O₃-n-Si
 × : negative bias on Al-(450 Å)Al₂O₃-p-Si

Measurements made with Au electrodes give approximately the same value of breakdown field as with Al electrode for positive bias on n-Si, but a value of 6.5MV/cm for negative bias on p-Si.

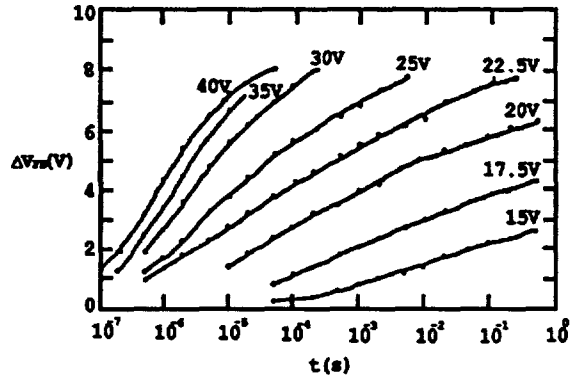


Fig.9. Flatband shift with log t for Al-(450 Å)Al₂O₃-n-Si with positive applied voltages as parameter

Fig.9 shows the results obtained by positive biasing a sample with an n-type substrate and Al electrodes. This graph demonstrates some typical features of the injection into Al₂O₃ layer. One can see from the curves that these are probably certain threshold biases below which almost no measurable flatband shift occurs for a given time.

Above this threshold bias, we observe a flatband shift as a function of the injection time. For applied voltages above the threshold bias, the flatband shift ΔV_{FB} can over a limited range, be written as approximately proportional to logarithm of the injection time, t. Over the range of applied voltage from 15V to 22.5V, the slopes of the curves are approximately the same. For $V_G > 22.5V$ the slopes of the curves increase with applied voltages. These curves suggest that there are three injection regions: a subthreshold region, an above threshold region in which $\Delta V_{FB} \propto \log t$ and a high field region which has a different injection mechanism.

Fig.10 shows the results obtained with negative bias on a sample with a p-type substrate and Al electrodes. This has the same general features shown in Fig.9.

Note that in both Fig.9 and Fig.10 the flatband shift is positive, indicating negative charging of the oxide. Note also that the

magnitude of the flatband shift is less for negative bias(Fig.10) than for positive bias(Fig.9).

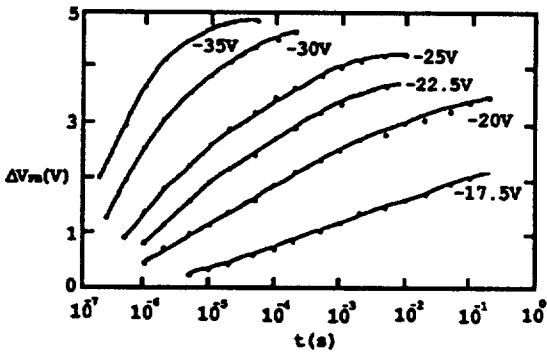


Fig.10. Flatband shift with log t for Al-(45 Å)Al₂O₃-p-Si with negative applied voltages as parameter

4. DISCUSSION OF EXPERIMENTAL RESULTS

The interpretation of the experimental studies of breakdown is facilitated by considering the band diagram of Fig.11. In Fig.11 we show the initial band configuration of the MOS capacitor under negative bias. If the applied field is greater than the threshold for injection, the electrons will be injected from the metal. In the recent papers, we know that, at least initially, these electrons will be trapped close to the metal. This produces the situation of Fig.11(b). The electron trapping has caused the field at the metal interface to diminish. This, in turn, reduces electron injection from metal.

Consequently, the current diminishes, as indicated in Fig.2 from Fig.11(b) we can see that, which the field at the metal interface decreases, the field at the semiconductor interface must increase to maintain the same average field. If the Si interface field is high enough, we may have (1)hole injection and trapping and/or (2)electron emission from donor centers in the oxide. It is either or both of these processes which cause the phenomenon of flatband voltage reduction under negative bias,

and we have the band bending shown in Fig.11(c). Note that since the Si interface field has now decreased, the field in the bulk of the oxide has increased. Hole injection and trapping will act to reduce the interface field : this is a self-quenching process.

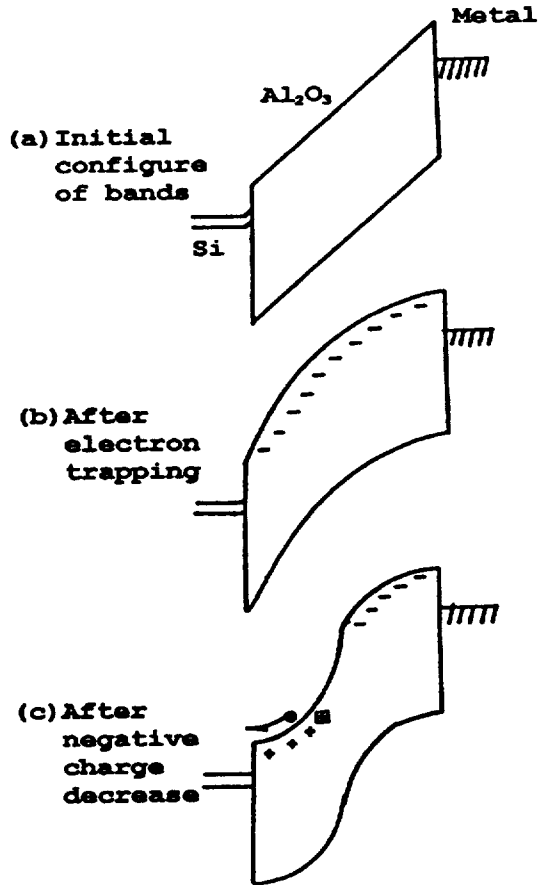


Fig.11. Model of electronic charging and breakdown mechanism;negative bias

Therefore, it cannot itself lead to breakdown. On the other hand, electron emission from donor centers in the bulk, which results in additional increase in the electric field. This process is thus unstable in the sense that once the critical field for electron emission is self-enhancing(positive feedback).

The current due to the enhanced electron emission from traps may not be large enough to produce a noticeable increase in the external

current until the field is very large. Then the current increase can be extremely rapid and can only be observed with a fast oscilloscope.

The model for breakdown with positive bias is similar, except that the interfaces in the above discussion are changed.

The absence of the flatband voltage decrease phenomenon can be easily explained. With positive bias, the electron injection and trapping occurs near the silicon interface, increasing the field at the metal interface. The electron emission from traps will therefore take place near the metal interface. Since the flatband voltage is proportional to the centroid of the trapped charge measured with respect to the metal interface, any positive charge near the metal can be masked by negative charge near the silicon, and there may not be any measurable flatband voltage decrease. Singh and Anand¹³⁾ have explained the difference in breakdown strength for negative and positive bias as due to the presence of positively charged surface states at the silicon interface.

The model which employs electron emission from traps rather than hole injection and trapping is also in good agreement with the results of a recent paper.¹⁴⁾

Impact ionization is probably not as significant in Al_2O_3 as it is in SiO_2 .^{15,16)} The mean free path is about 10\AA , as compared to about 34\AA for SiO_2 . This implies that, if impact ionization were the dominant breakdown mechanism, we would observe a much higher breakdown strength in Al_2O_3 than in SiO_2 . This is not the case. Also, in SiO_2 a current multiplication effect is observed prior to breakdown. This is a steady increase in the current which occurs over a period of seconds to minutes. No such effect was seen in Al_2O_3 . Finally, if impact ionization were important, the breakdown strength should decrease as one goes to low temperatures because the mean free path increases at lower temperature. However, an increase, rather than a decrease, in the breakdown strength of Al_2O_3 is observed at low temperatures.¹²⁾ These results make impact ionization seen unlikely to be of importance in

the breakdown of Al_2O_3 .

5. CONCLUSIONS

Aluminum oxide(Al_2O_3) offers some unique advantages over the conventional silicon dioxide(SiO_2) gate insulation; possibility of obtaining low threshold-voltage MOSFETs, and possibility of use as in nonvolatile memory devices. We have undertaken a study of the high-field properties of Al_2O_3 on Si deposited by GAIVBE Technique.

Our test structures were metal-aluminum oxide-silicon capacitors with both aluminum and gold field plates. The major problem with Al_2O_3 , when used as a gate insulator, is its flatband voltage instability under moderate bias levels($>1\text{MV/cm}$).

This is caused by trapping of electrons in the oxide.

We have explored the mechanism of charge injection and trapping from both a theoretical and an experimental viewpoint.

In this paper, the dielectric breakdown of Al_2O_3 was also studied. It was found that, because of the continuous buildup of space charge, a consistent determination of breakdown strength could not be made using a ramp voltage waveform. Instead, a study was done of the time to breakdown for a given fixed bias. The average fields required to produce breakdown in 10^3sec were approximately 4.5MV/cm for positive bias on either Al or Au field plates, 5.0MV/cm for negative bias on Al, and 6.5MV/cm for negative bias on Au. These fields correspond to the threshold for the onset of the high field conduction mechanism. Thus, we have additional support for the model in which instability is brought about by field emission of electrons from initially neutral centers, thus producing positive space charge near the positive interface. Hole injection through this interface, followed by trapping, would be a self-limiting process, whereas the buildup of space charge caused by field emission would tend to cause further field emission.

We investigated the physical damage produced by breakdown. The use of thin (200Å and 1,000Å) Al and Au field plates made this possible. With Au field plates, we observed self-quenched break-downs(SQBDs) before the final shorting breakdown. With Al field plates, we never observed SQBDs. We conjecture that this might be due to the difference in the bonding properties of Au and Al to Al₂O₃.

Another phenomenon that we observed was an apparent edge effect, the majority of breakdown sites occurring in samples with Al field plates were located at or near the edge of the field plate. This effect was particularly noticeable in samples with square field plates, where the breakdown sites were frequently to be found at the corners of the field plates, as might be expected from the field enhancement there.

6. ACKNOWLEDGEMENTS

The authors are grateful to Inter-University Semiconductor Research Center, Seoul National University for the interest in this work and continual encouragement.

This work was supported by the Ministry of Education through Grant No. ISRC-94-E-1015. (Semiconductor Fields)

REFERENCE

- 1) N.M.Johnson and M.A.Lampert, "Electron trapping in aluminum implanted silicon dioxide films on silicon", *J.Appl.Phys.*, vol.46, pp. 1216~1222, March 1975.
- 2) S.M.Sze, *Physics of Semiconductor Devices*, 2nd Edition, John Wiley and Sons.Inc., 1985, ch. 8.
- 3) E.H.Nicollian and C.N.Berglund, "Avalanche injection of electrons into insulating SiO₂ using MOS structures", *J.Appl.Phys.*, vol.41, pp. 3052~3057, June 1970.
- 4) D.J.DiMaria, J.M.Aitken and D.R.Young, "Capture of electrons into Na⁺-related trapping sites in the SiO₂ layer of MOS structures at 77 °K", *J.Appl.Phys.*, vol 47, pp. 2740~2743, June 1976.
- 5) W.S.Johnson and J.H.Gibbons, *Projected Range Statistics Semiconductors and Related Materials*, 2nd Edition, John Wiley and Sons.Inc.,1975, ch. 5.
- 6) R.H.Walden, "A method for the determination of high-field conduction laws in insulating films in the presence of charge trapping", *J.Appl.Phys.*, vol.43, pp. 1178~1186, March 1972.
- 7) L.F.Mondolfo, *Aluminum Alloy-Structure & Properties*, Butterworth CO.LTD., 1976, ch. 1.
- 8) Kiyoto Linda and Tohru Tsujide, "Physical and chemical properties of aluminum oxide film deposited by AlCl₃-CO₂-H₂ system", *Jap. J.Appl.Phys.*, vol.11, pp. 840~849, June 1972.
- 9) D.A.Mehta, S.R.Butler and F.J.Feigl, "Effect of postdeposition annealing treatment on charge trapping in CVD Al₂O₃ films on Si", *J.Electrochem.Soc.*, vol.120, pp. 1707~1714, December 1973.
- 10) M.Y.Sung et al, *15th Int.Conf.on Metallurgical Coatings and 1988 Vacuum Metallurgy Conf.on Special Meeting*, San Diego, CA, April 11~15, 1988.
- 11) M.Y.Sung et al, *35th National Symposium American Vacuum Society*, Atlanta, GA, Oct.3~7, 1988.
- 12) T.Tsujide, S.Nakanuma and Y.Ikushima, "Properties of aluminum oxide obtained by hydrolysis of AlCl₃", *J.Electrochem.Soc.*, vol.117, pp. 703~708, May 1970.
- 13) S.Singh and K.V.Anand, "Electrochemical properties of dielectric films of aluminum oxide deposited on Si", *Thin Sol.Films*, vol.37, pp. 453~460, 1976
- 14) J.J.O'Dwyer, *The Theory of Electrical Conduction and Breakdown in Solid Dielectrics*, Clarendon Press, Oxford., 1973, pp. 20~47.
- 15) F.B.Mclean and P.S.Windour, "Rapid annealing and charge injection in Al₂O₃ MIS capacitors", *IEEE Tran.Nucl.Sci.*, NS-21, pp. 47~53 1974.
- 16) J.A.Aboaf, "Deposition and properties of aluminum oxide obtained by pyrolytic deco-

- composition of an aluminum alkoxide”, *J. Electrochem.Soc.*, vol.114, pp. 948~952, September 1967.
- 17) M.Y.Sung and B.Cowell, "Growth of GaAs on Si using Ionized Cluster Beam Technique”, *J.of Vacuum Science and Technology*, vol.A-7(3), pp. 792~795, 1989.
- 18) N.Klein, *Electrical Breakdown in Solids*, Academic Press, New York, 1969, ch. 3.
- 19) C.N.Berglund and R.J.Powell, "Photoinjection into SiO₂: Electron scattering in the image force potential well”, *J.Appl.Phys.*, vol.42, pp. 573~577 February 1971.

저자소개

성만영



1949년 6월 3일생. 1974년 고려대학교 전기공학과 졸업. 1981년 동 대학원 졸업(공학). 1985년 Univ. of Illinois 부교수. 현재 고려대학교 전기공학과 교수.

김태익



1967년 8월 19일생. 1991년 고려대학교 공대 전기공학과 졸업. 현재 동 대학원 석사과정.

문병무



1956년 4월 25일생. 1982년 고려대학교 전기공학과 졸업. 1985년 미국 Rutgers대학(석사). 1990년 미국 Rutgers대학(공학박). 1991년 Univ. of Illinois(UC) Post Doc. 1992년 Royal Institute of Technology(Sweden) 연구교수. 1994년 현재 고려대학교 전기공학과 조교수.

K. V. Rao



1967년 Oxford 물리학박사. 1978-1980년 Univ. of Illinois 부교수. 1980-1984년 3M Research Lab. 1984년- 현재 Royal Institute of Technology(Sweden) 교수.

박성희



1935년 4월 11일생. 1966년 명지대 공대 전기공학과 졸업. 1987년 단국대학교 공학박사. 1979년- 현재 호서대학교 전자공학과 교수.